ChemPubSoc Europe

DOI: 10.1002/open.201600174

Open Access ChemistryOPEN Communications

Novel 5-(Benzo[b]thiophen-3-yl)pyridine-3-carbaldehyde (BTPA) Functionalization Framework For Modulating Fullerene Electronics

Suru V. John,[a] Christian C. De Filippo,[b] Simone Silvestrini,[b] Michele Maggini,[b] and Emmanuel Iwuoha*[a]

Through a cycloaddition reaction, fullerene (C_{60}) was derivatized with a novel organic compound 5-(benzo[b]thiophen-3-yl)pyridine-3-carbaldehyde to form the processable and stable 3-(benzo[b]thiophene-3yl)-5-fullero-1-methylpyrrolidinepyridine (BTFP) compound. BTFP exhibits close similarities to phenyl-C61-butyric-acid-methyl-ester (PCBM) in terms of first reduction potential values (−0.62 and −0.61 V vs. Ag/AgCl, for BTFP and PCBM, respectively) and lowest occupied molecular orbital (LUMO) energy level values (3.93 eV in both cases). In chloroform, BTFP exhibits a bathochromic shift in the λ_{max} of BTFP (λ_{max}BTFP = 290 nm and λ_{max}PCBM = 260 nm), owing to the grafted benzo[b]thiophene-3-yl)pyridine moiety. Despite the similarity in LUMO (3.93 eV) energy values, BTFP and PCBM differ in their luminescence-quenching ability. The bathochromic shift in the λ_{max} of BTFP (relative to PCMB) is likely to contribute to improved light absorption of a suitable donor for photovoltaic applications.

The uniqueness of closed-cage, nearly spherical C_{60} and related fullerene molecules has attracted considerable attention. The icosahedral symmetry[1] and numerous possibilities of functionalization allow the modulation of their optoelectronic properties,[2] leading to unabated interest in these intriguing carbon allotropes. The chemistry of fullerenes is that of electron-poor olefins, with sp^2 carbon atoms constrained into a pyramidalized geometry. Multiple double bonds are available on the carbon backbone, making multiple functionalization[3] an interesting route towards new functional materials. This has led to a variety of novel compounds with finely tunable features that have found applications as catalysts[4] and antioxidants,[5] as well as in sensors[6] and solar cells.[2a,7] The functionalization of fullerenes does not only modify their properties, but converts them into more processable forms, as pristine C_{60} is only sparsely soluble in most solvents, making it intractable. Indeed, the quest for soluble fullerenes was (and still is) one of the main driving forces in the field of covalent modification of carbon nanostructures. Phenyl-C61-butyric-acid-methyl-ester (PCBM), a fullerene derivative, is a solution-processable n-type organic semiconductor, which is commonly blended with p-type conjugated polymers to make photovoltaic (PV) cells. However, owing to the dependence of PV properties on frontier orbital energy levels of donor and acceptors, the application of PCBM to all donor polymers irrespective of their optoelectronic properties leads to untrue PV properties. For instance, reports by Susarova et al.[8] and Kästner et al.[9] compared the PV responses of a set of polymers with PCBM and other functionalized fullerenes and observed that PCBM gave just moderate efficiencies in combination with the polymers, whereas the best PV performances were obtained with a blend of each polymer with specific fullerene derivatives possessing better-suiting molecular structures. Herein, we describe a fulleropyrrolidine,[10,11] 3-(benzo[b]thiophene-3yl)-5-fullero-1-methylpyrrolidinepyridine (BTFP), which is obtained from C_{60} through 1,3-dipolar cycloaddition of the azomethine ylide formed when 5-(benzo[b]thiophen-3-yl)pyridine-3-carbaldehyde (BTPA) reacts with sarcosine. Besides the structural characterization of BTFP, we report its electrochemical and spectroscopic properties to assess its potential as an electron-acceptor material for organic PV cells. The PV cell performances of blends of BTFP with two electron-donating polymers, poly(9,9-dioctylfluorene-2,7-diyl-alt-benzo[2,1,3]thiadiazole-4,7-diyl) (F8BT) and poly(9,9-dioctyl-fluorene-2,7-diyl-alt-2,2′-bithiophene-5,5′-diyl) (F8T2), were evaluated and compared with PCBM.

The synthetic routes leading to the preparation of BTPA and BTFP are shown in Scheme 1 and Scheme 2, respectively. The products were characterized by NMR (see the Supporting Information), UV/Vis, photoluminescence, TEM, and SEM/EDS. For BTPA, ^{1}H NMR in [D_6]DMSO confirmed the presence of aldehyde at 10.2 ppm (Figures S1 and S2), whereas ^{13}C NMR showed 14 signals, as expected for the proposed structure (Figures S3 and S4). Mass spectrometry confirmed the product at m/z = 240.04, whereas m/z = 258.05 corresponds to the hydrated product [$M + H_2O$] (Figure S5). The product is bright yellow, stable, and soluble in common organic solvents, for example dichloromethane, chloroform, and toluene, as investigated. The ^{13}C NMR spectrum of BTFP shows the loss of an al-

[a] S. V. John, Prof. E. Iwuoha
SensorLab, Department of Chemistry
University of Western Cape
Robert Sobukwe Road, Bellville
Cape Town 7535 (South Africa)
E-mail: eiwuoha@uwc.ac.za

[b] Dr. C. C. De Filippo, Dr. S. Silvestrini, Prof. M. Maggini
Chemical Sciences Department
University of Padova
Via Marzolo 1 35131, Padova (Italy)

Supporting Information and the ORCID identification number(s) for the author(s) of this article can be found under http://dx.doi.org/10.1002/open.201600174.

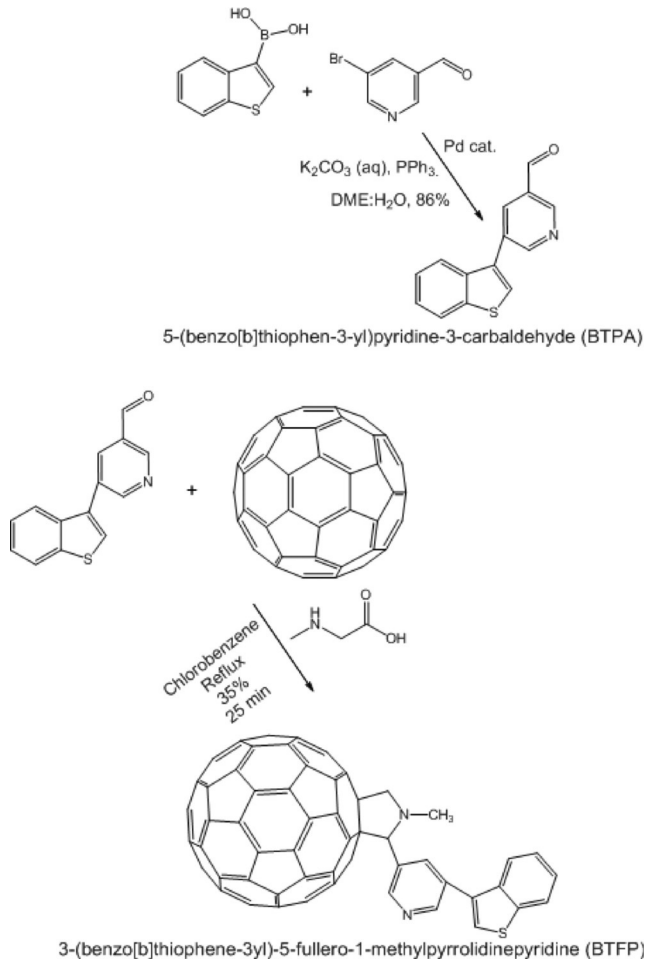

Scheme 1. Synthesis of BTPA and BTFP.

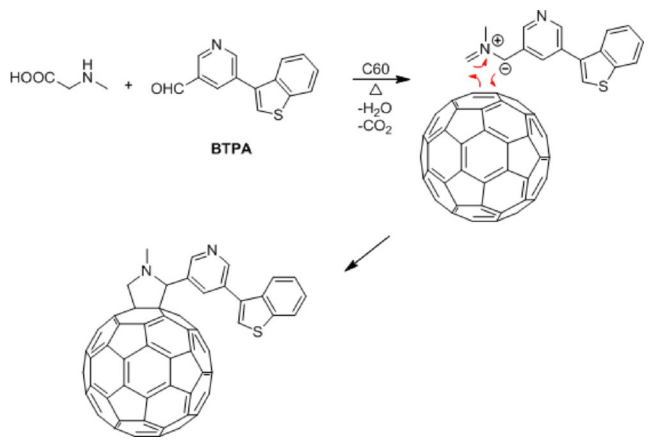

Scheme 2. Mechanism for the synthesis of BTFP.

dehyde (at 188 ppm) from BTPA, along with the splitting of the C_{60} signal (141 ppm) into 10 signals in the 140–145 region, owing to the breaking of the spherical symmetry of the starting material (Figure S7). The results show a shift and slight distortion of the BTFP geometry in relation to C_{60} and BTPA. DEPT data (Figure S8) show the signals for the *N*-methyl glycine analogue, demonstrating that we have an *N*-CH_3 (at 37.9 ppm), a $-CH_2$ (at 68.3 ppm), and a $-CH$ signal (at 79.3 ppm), owing to the linkage between the glycine and the BTPA (where the BTPA contributed the C). The ^1H data also show the loss of the aldehyde signal when forming the conjugate (Figure S9). ^1H NMR spectra show the $-CH_2$ protons of the pyrrolidine ring as two doublets ($J = 9.6$ Hz) at 4.37 and 5.05 ppm, and a $-CH$ proton singlet at 5.14 ppm (Figure S10). Protons of the methyl group ($-CH_3$) attached to the nitrogen atom of the pyrrolidine ring appear as a singlet around 2.86 ppm.

FTIR of BTPA (Figure 1) confirms the presence of the pyridine ring and the carbonyl group with stretching frequencies at 1650 and 1696 cm^{-1}, respectively. BTFP, on the other hand, did

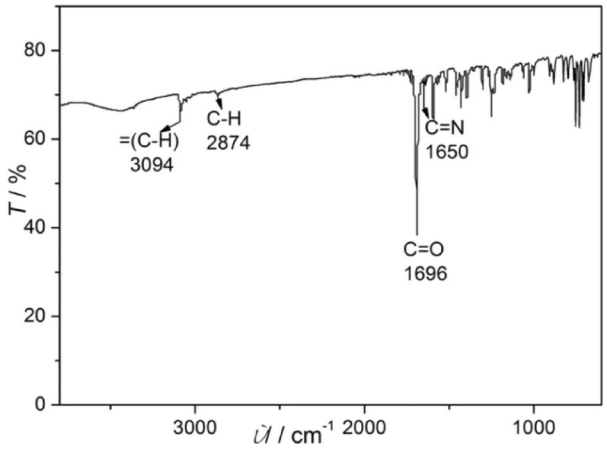

Figure 1. FTIR spectrum of BTPA.

not yield any signal for the carbonyl group, whereas pyridine signals are still present, albeit weak (Figure S12), thereby hinting at the success of the cycloaddition reaction. Prominent fullerene C_{60} IR-active peaks at 527 and 577 cm^{-1}, associated with the primary radial motion of the carbon atoms, as well as at 1184 and 1426 cm^{-1}, associated with the tangential motion of the carbon atoms,[4a,12] were also observed in BTFP.

Figure 2 shows the morphology of BTPA crystals, as observed by using SEM. The product shows a needlelike mor-

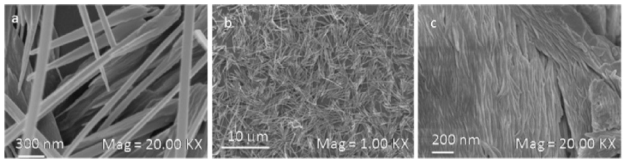

Figure 2. High-resolution SEM images of BTPA: a) thin film at 20 000× magnification, b) thin film at 1000× magnification, and c) powder sample.

phology and its EDS spectrum analysis (Figure 3) is compatible with the structure of the compound. EDS analysis of BTFP (Figure 4) also corresponds to the structure with 93.72% C, 5.18% N, and 1.1% S. Furthermore, a comparison between the morphologies of molecular crystals of [60]fullerene, BTPA, and BTFP is made by using SEM and TEM in Figure 5 and Figure 6,

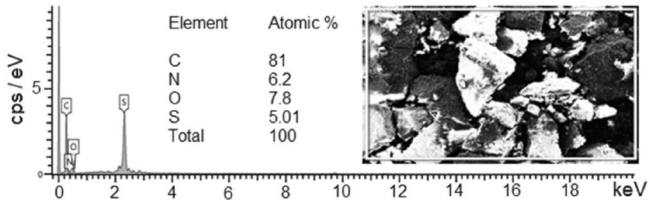

Figure 3. EDS spectrum of BTPA.

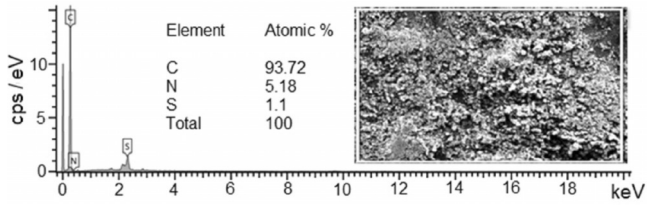

Figure 4. EDS spectrum of BTFP.

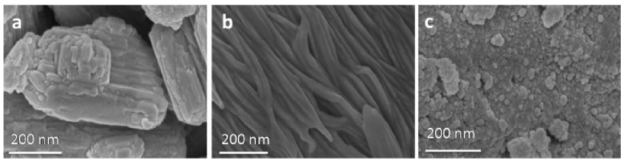

Figure 5. High-resolution SEM images of a) fullerene C_{60}, b) BTPA, and c) BTFP at 50 000 magnification.

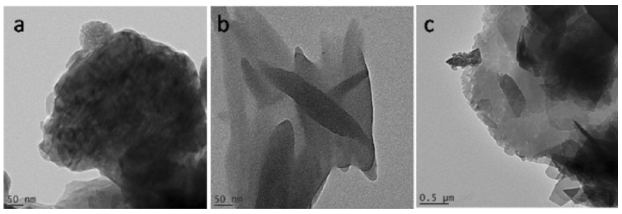

Figure 6. High-resolution TEM images of a) fullerene C_{60}, b) BTPA, and c) BTFP.

respectively. The SEM and TEM images show the BTFP morphology to be similar to the morphology of a combination of C_{60} and BTPA. These analyses, in a way, also confirm the successful synthesis of BTFP.

The UV/Vis spectrum of BTPA (Figure 7) is dominated by the $\pi \rightarrow \pi^*$ transition. The spectra of BTFP in dichloromethane and chloroform are shown in Figure 8 (a and b, respectively), and are compared to PCBM. Similar to PCBM, the electronic spectra of BTFP is dominated by the $\pi \rightarrow \pi^*$ transitions with strong absorption in the UV region, which corresponds to the allowed electronic transition in the fullerene core.[13]

In dichloromethane, the two spectra show analogous absorptions, except for the rise of a peak ("peak a") at approximately 310 nm for BTFP. The situation changes in chloroform, where BTFP displays a positive solvatochromism with two structured peaks located at 290 and 307 nm, and a shoulder at 329 nm. The absorptions of BTFP in dichloromethane located

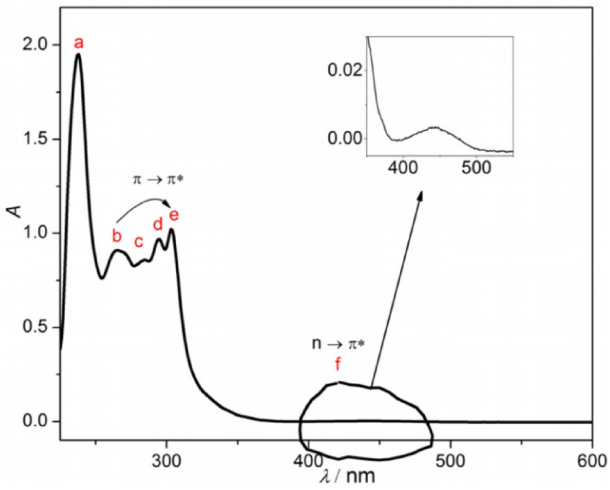

Figure 7. UV/Vis spectrum of BTPA in dichloromethane. Inset is the visible-region absorption.

at 256, 310, and 430 nm show typical features characteristic of a mono-fulleropyrrolidine derivative.[14]

The absorption responses of BTFP and PCBM (as acceptors) were investigated in thin-film blends with donor materials. Donors and donor–acceptor blends were investigated in thin films prepared from chloroform solution. For donors, we employed F8BT and F8T2. Materials were dissolved in chloroform, cast onto pre-cleaned glass slides and dried under argon prior to measurements. For donor–acceptor blends, films were cast from a 1:1 blend ratio. Film thicknesses ranged from 90 to 130 nm. Figure 8c shows the spectra of the investigated donors and donor–acceptor blends. The maximum wavelengths of absorption of the donor (F8BT and F8T2) and donor–acceptor blends (F8BT:BTFP, F8BT:PCBM, F8T2:BTFP, and F8T2:PCBM) are observed in the visible region of the electromagnetic spectrum. However, a bathochromic shift is observed for donor–acceptor blends with BTFP as the acceptor and with an interesting emerging peak at around 550 nm for both donors. This peak is not present in the absorption spectra of F8BT and F8T2, and it is also absent in the blends of F8BT:PCBM and F8T2:PCBM. This property displayed by BTFP is capable of enhancing the photophysical properties when blended with a suitable donor, thereby enhancing PV device performance.

To investigate the electron-accepting properties of BTFP, the photoluminescence spectra of donor–acceptor blends were assayed. For donors, we also employed F8BT and F8T2. BTFP was used as the acceptor and was compared to PCBM. Samples were prepared as described for the sample preparation for thin-film absorption measurement.

The photoluminescence responses of F8BT and F8T2 samples blended with PCBM and BTFP were measured at excitation wavelengths of 450 and 458 nm for blends based on F8BT and F8T2, respectively. To compare the degree of photoluminescence quenching, the fluorescence spectra of pristine F8BT and F8T2 films were measured as controls. Photoluminescence quenching is described by the ratio of the emission intensity

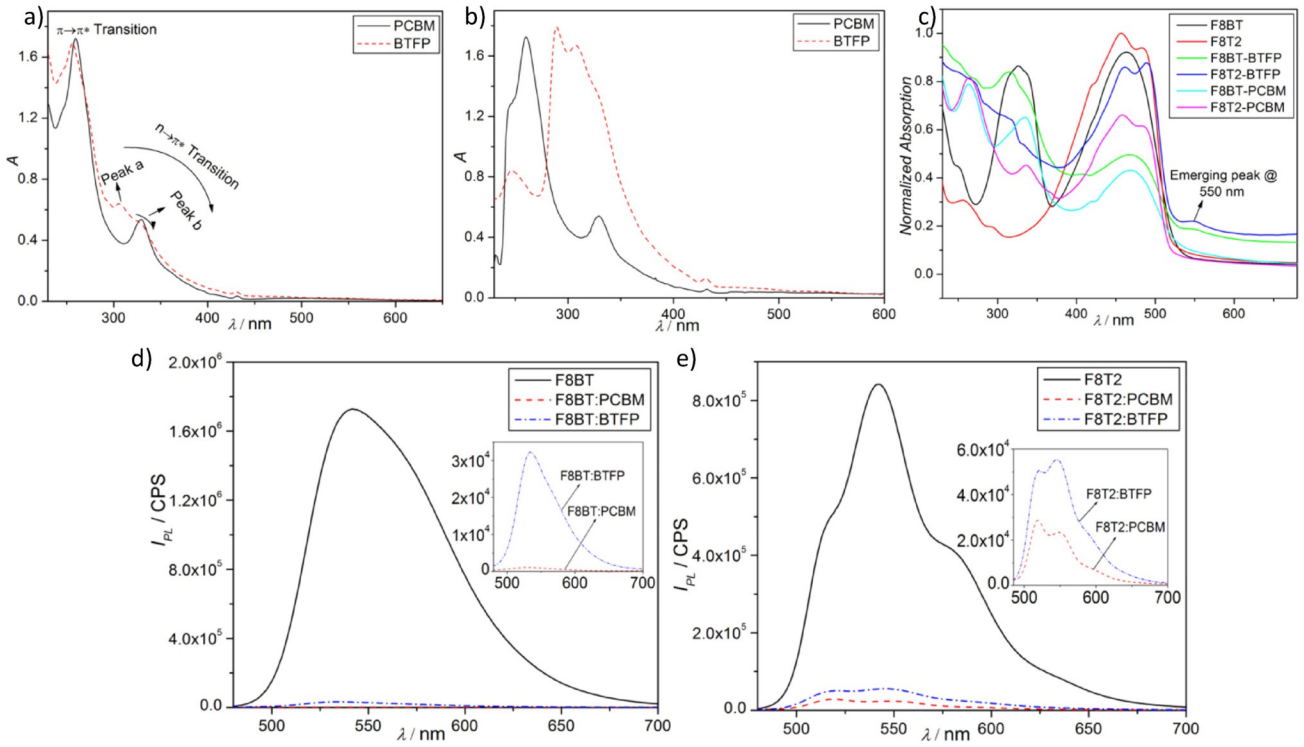

Figure 8. a) UV/Vis spectra of BTFP and PCBM in dichloromethane. b) UV/Vis spectra of BTFP and PCBM in chloroform. c) UV/Vis spectra of F8BT, F8T2, F8BT:BTFP (1:1), F8T2:BTFP (1:1), F8BT:PCBM (1:1), and F8T2:PCBM (1:1) in thin films prepared from chloroform. d) Photoluminescence quenching spectra of F8BT [donor–acceptor blend ratio (1:1)]. e) Photoluminescence quenching spectra of F8T2 [donor–acceptor blend ratio (1:1)].

of the polymer/fullerene blend normalized over the emission intensity of the pristine polymer. The photoluminescence quenching of both acceptors differs, as can be seen in Figures 8 d and 8 e (inset). The quenching of donor F8BT and F8T2 blended with PCBM and BTFP acceptors in separate experiments decreased in the order PCBM > BTFP. The reduced quenching observed for BTFP relative to PCBM can be attributed to the inability of BTFP to properly mix with the investigated donors as a result of the solubility challenge of BTFP. In this situation, the distance between the donor and acceptor interfacial layer is likely to increase, thereby increasing the distance the electrons will have to travel. The ability of the acceptor to accept released electrons from the donor is, therefore, hindered and, as a result, its quenching potential is not optimum.

The redox behavior of BTFP with that of the parent C_{60} and PCBM was determined by using cyclic voltammetry (CV) under identical conditions [e.g. V vs. Ag/AgCl, $TBAF_6P$ (0.1 M) as supporting electrolyte, 1,2-DCB/MeCN (4:1) as the solvent, 100 mV s^{-1}, and a glassy carbon electrode (GCE) as the working electrode]. The cyclic voltammograms (Figure 9) show four reversible reduction waves (**a**–**d** in the range −2.2 to 0 V vs. Ag/AgCl), corresponding to the reduction of the fullerene cage. As shown in the Table 1, the voltammograms of PCBM and BTFP show a cathodic shift in all well-defined reduction waves in comparison to C_{60}. Both systems show identical cathodic shifts for reduction potentials **a** and **b,** whereas **c** showed a slight difference. The voltammogram showed a comparable first reduction wave for PCBM and BTFP with a distinctive difference in comparison to C_{60}. The first reduction wave is indicative of

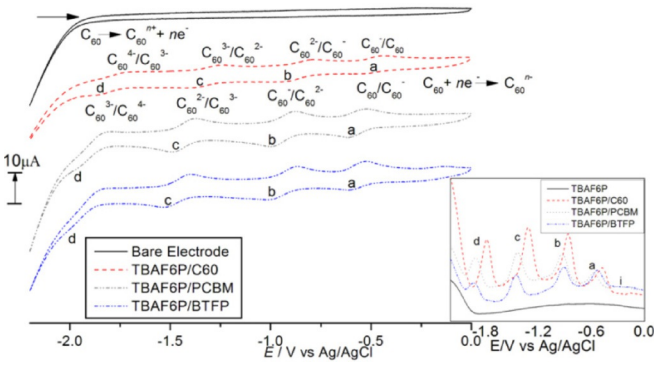

Figure 9. CV of C_{60}, PCBM, and BTFP in $TBAF_6P$ with a GCE at 50 mV s^{-1}. Inset shows the SWV.

Table 1. Cathodic shifts of PCBM and BTFP in relation to reduction potentials of C_{60}.

	Cathodic shift [V vs. Ag/AgCl]			E_{red}^{on}	LUMO
	a	**b**	**c**	[V]	[eV]
C_{60}				−0.29	4.11
PCBM	0.21	0.10	0.15	−0.47	3.93
BTFP	0.22	0.10	0.22	−0.47	3.93

Experimental conditions: $TBAF_6P$ (0.1 M) as supporting electrolyte; 1,2-DCB/MeCN (4:1) as the solvent; 100 mV s^{-1}; GCE as the working electrode.

the electron-acceptor strength of the compounds. C_{60} (±0.50 V) appeared to be a better electron acceptor than PCBM (±0.61 V) and BTFP (±0.62 V), and there is the possibility of electron transfer with PCBM and BTFP, owing to the cathodic shifts. The square wave voltammetry (SWV), on the other hand, revealed five peak potentials for C_{60}, PCBM, and BTFP [Figure 9 (inset)]. These peak potentials and their relative cathodic shifts are well defined in the SWV when using Pt as the working electrode (Figure 10). The SWV better resolved

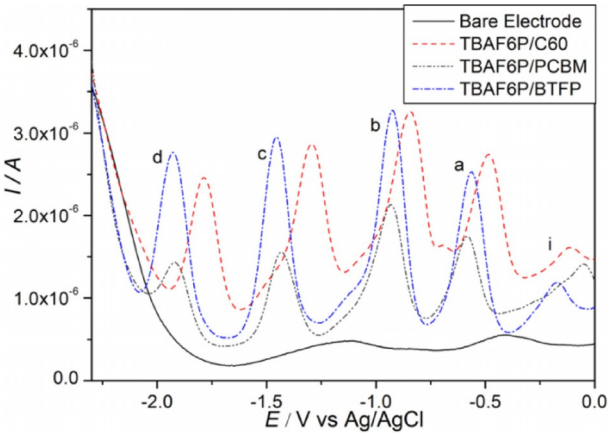

Figure 10. SWV of PtE, C_{60}, PCBM, and BTFP.

peak **d** and revealed a new signal, peak **i**, for C_{60}, PCBM, and BTFP. The onset reduction potentials E_{red}^{on} were estimated at the potential at which the current response begins to deviate from the baseline, recording −0.47 for both PCBM and BTFP. From the E_{red}^{on}, the LUMO energy levels were calculated according to the equation $-(E_{red}^{on} + 4.4)$ eV.[15] The result shows both PCBM and BTFP to be energetically identical.

Several studies into the electrochemical properties and behavior of C_{60} with 3- to 6-electron reduction, depending on the solvent, supporting electrolyte, and temperature of reaction, have been reported (Table S2). These studies show that the choice of solvent, supporting electrolyte, temperature, and other factors have a profound effect on the value of the reduction potential of fullerenes. Therefore, one should compare the relative differences in those potentials, rather than evaluate their absolute values.

In conclusion, a novel organic compound (BTPA) with a nanostructured morphology was synthesized and applied for the extremely rapid functionalization of C_{60} to obtain a processable fullerene derivative (BTFP). BTFP showed interesting photophysical absorptive properties in solution and thin films. When blended with the investigated donors, F8BT and F8T2, a bathochromic shift coupled with a new peak at longer wavelengths were observed for the blends compared to blends with PCBM as the acceptor. This is likely to enhance the PV performance of a suitable donor. The study, however, revealed PCBM and BTFP to exhibit about the same first reduction potential in (0.1 M) $TBABF_6$ supporting electrolyte (−0.61 and −0.62 V vs. Ag/AgCl, respectively) with a LUMO of 3.93 eV in both cases. This makes BTFP energetically PCBM-like. Nonetheless, they differ in their luminescence properties. Although the solubility of this material needs to be improved, it shows promise for electronic applications and may contribute to the development of new technologies. Efforts to improve the solubility are underway and achieving this will make BTFP compete with PCBM, with advantages of cost and ease of synthesis.

Experimental Section

All starting materials and solvents were purchased from Sigma Aldrich and used as received. A detailed synthesis procedure is given in the Supporting Information.

Acknowledgements

The authors acknowledge the National Research Foundation of South Africa and the Coimbra Group of Universities for scholarships and financial support.

Conflict of Interest

The authors declare no conflict of interest.

Keywords: azomethine ylides · cycloaddition · electrochemistry · fullerenes · photoluminescence

[1] M. Bodner, J. Patera, M. Szajewska, *PLoS One* **2014**, *9*, 1–5.
[2] a) Y. Liu, X. Du, J. Cao, W. Zhang, S. Chen, Z. Xiao, X. Cai, Q. Zuo, L. Ding, *Synth. Met.* **2012**, *162*, 1271–1278; b) K. Lewandowska, B. Barszcz, A. Graja, A. Biadasz, B. Bursa, D. Wróbel, S.-T. Kim, T.-D. Kim, K.-S. Lee, *Synth. Met.* **2012**, *162*, 2134–2137; c) M. Lehmann, M. Hîgel, *Angew. Chem. Int. Ed.* **2015**, *54*, 4110–4114; *Angew. Chem.* **2015**, *127*, 4183–4187; d) L. Moreira, J. Calbo, B. M. Illescas, J. Arago, I. Nierengarten, B. Delavaux-Nicot, E. Orti, N. Martin, J.-F. Nierengarten, *Angew. Chem. Int. Ed.* **2015**, *54*, 1255–1260; *Angew. Chem.* **2015**, *127*, 1271–1276.
[3] M. Anafcheh, R. Ghafouri, *Phys. E* **2014**, *56*, 351–356.
[4] a) H. Veisi, R. Masti, D. Kordestani, M. Safaei, O. Sahin, *J. Mol. Catal. A J. Mol. Catal. A: Chem.* **2014**, *385*, 61–67; b) X. Zhang, Q. Wang, L.-H. Zou, J.-W. You, *J. Colloid Interface Sci. J. Col. Interf. Sci* **2016**, *466*, 56–61.
[5] J. Vávrová, M. Řezáčová, J. Pejchal, *J. Appl. Biomed.* **2012**, *10*, 1–8.
[6] a) Y.-F. Gao, T. Yang, X.-L. Yang, Y.-S. Zhang, B.-L. Xiao, J. Hong, N. Sheibani, H. Ghourchian, T. Hong, A. A. Moosavi-Movahedi, *Biosens. Bioelectron.* **2014**, *60*, 30–34; b) S. Afreen, K. Muthoosamy, S. Manickam, U. Hashim, *Biosens. Bioelectron.* **2015**, *63*, 354–364; c) X. Danga, C. Hub, H. Chen, J. Huang, D. Zheng, S. Hu, *Sens. Actuators B* **2016**, *228*, 709–715.
[7] S. Urnikaite, T. Malinauskas, V. Gaidelis, R. Maldzius, V. Jankauskas, V. Getautis, *Carbon* **2011**, *49*, 320–325.
[8] D. K. Susarova, E. A. Khakina, P. A. Troshin, A. E. Goryachev, N. S. Sariciftci, V. F. Razumov, D. A. M. Egbe, *J. Mater. Chem.* **2011**, *21*, 2356–2361.
[9] C. Kästner, C. Ulbricht, D. A. M. Egbe, H. Hoppe, *J. Polym. Sci. Part B* **2012**, *50*, 1562–1566.
[10] a) F.-F. Li, J. R. Pinzón, B. Q. Mercado, M. M. Olmstead, A. L. Balch, L. Echegoyen, *J. Am. Chem. Soc.* **2011**, *133*, 1563–1571; b) E. E. Maroto, A. d. Cozar, S. Filippone, A. Martin-Domenech, M. Suarez, F. P. Cossio, N. Martin, *Angew. Chem.* **2011**, *123*, 6184–6188; c) J. Marco-Martínez, V. Marcos, S. Reboredo, S. Filippone, N. Martin, *Angew. Chem. Int. Ed.* **2013**, *52*, 5115–5119; *Angew. Chem.* **2013**, *125*, 5219–5223; d) S. Sato, Y. Maeda, J.-D. Guo, M. Yamada, N. Mizorogi, S. Nagase, T. Akasaka, *J. Am. Chem. Soc.* **2013**, *135*, 5582–5587.
[11] M. Maggini, G. Scorrano, M. Prato, *J. Am. Chem. Soc.* **1993**, *115*, 9798–9799.

[12] S. Iglesias-Groth, F. Cataldo, A. Manchado, *Mon. Not. R. Astron. Soc.* **2011**, *413*, 213 – 222.
[13] K. Kordatos, T. D. Ros, M. Prato, R. V. Bensasson, S. Leach, *Chem. Phys.* **2003**, *293*, 263 – 280.
[14] a) P. Zhang, Z. X. Guo, S. Lv, *Chin. Chem. Lett.* **2008**, *19*, 1039 – 1042; b) A. Parveen, V. Sughanya, S. Nagarajan, *Spectrochim. Acta Part A* **2016**, *152*, 77 – 81.
[15] S. Admassie, O. Inganas, W. Mammo, E. Perzon, M. R. Andersson, *Synth. Met.* **2006**, *156*, 614 – 623.

Received: December 30, 2016
Version of record online April 4, 2017

